

Cite this article as: Wu Xiaodong, Wang Lianjin, Wang Zhongying, et al. Effect of La and Ce on High Temperature Oxidation Behavior of Fe25Cr5Al Alloys[J]. Rare Metal Materials and Engineering, 2021, 50(11): 3837-3844.

ARTICLE

Effect of La and Ce on High Temperature Oxidation Behavior of Fe25Cr5Al Alloys

Wu Xiaodong¹, Wang Lianjin¹, Wang Zhongying², Chen Xueqin¹, Wang Shuang¹

¹ School of Materials Science and Engineering, Jiangsu University, Zhenjiang 212000, China; ² Huai'an CIRSI Co., Ltd, Huai'an 223000, China

Abstract: Fe25Cr5Al alloys with and without rare earth (RE) elements La and Ce, namely Fe25Cr5Al-RE and Fe25Cr5Al alloys, were prepared and isothermal oxidation tests were conducted at 1100 °C. The morphology of oxide scale was observed by scanning electron microscope (SEM), and the oxidation product was identified by energy disperse spectroscopy (EDS) coupled with X-ray diffraction (XRD). Results show that after oxidation for 1, 20, and 300 h, the mass gain of Fe25Cr5Al alloys is 0.08, 0.84, and 4.41 mg·cm⁻², but that of Fe25Cr5Al-RE alloys is 0.03, 0.35, and 0.92 mg·cm⁻², respectively. The oxide scale of the two alloys consists of α -Al₂O₃. La and Ce promote the formation of compact and continuous oxide scale, which significantly improves the high temperature oxidation resistance of Fe25Cr5Al alloys. Moreover, RE oxide pegs can be observed at substrate/scale interface of Fe25Cr5Al-RE alloys, which makes the bond between substrate and scale tighter, thus enhancing the adhesion of the interface. There are RE oxides in oxide scale of Fe25Cr5Al-RE alloys, which effectively inhibits further oxidation of the alloys.

Key words: oxidation mechanism; Fe25Cr5Al alloys; oxide scale

Fe-Cr-Al alloys have a great potential in research and application because of their oxidation and corrosion resistance with a low expansion coefficient. They have been employed for automobile exhaust gas purifying system^[1,2], fuel cladding material^[3,4], and electrothermal alloy material^[5]. However, under severe conditions such as thermal fatigue and thermal shock, the oxide scale wrinkles, cracks, and even falls off, resulting in a sharp drop in the high temperature oxidation resistance of the alloy, which is the main factor leading to the failure of the material system^[6-8]. Rare earth (RE) elements such as Hf, Y, La, and Ce have been used to improve the oxidation resistance and scale adhesion of many superalloys^[9-12]. However, the effects of RE elements on the strength of the substrate and the oxide scale and the growth mechanism of the oxide scale are still ambiguous, and there are different perspectives.

The major perspectives of the influence mechanism of RE elements on the oxidation resistance of heat-resistant alloys can be summarized as follows. (1) Oxide pegs are formed at scale/substrate interface during the high-temperature oxidation process. The RE elements in alloys are internally oxidized to

form oxide pegs which provide rapid ion diffusion channels and facilitate oxide scale to grow around the oxide pegs. Meanwhile, due to the large atomic radius of RE elements, RE elements tend to segregate at the grain boundary, and the reduction of grain boundary energy promotes the oxide scale growth from the grain boundary, thus forming the grain boundary oxide pegs^[13-16]. (2) Prevent the lateral growth of the oxide scale. The oxidation mechanism of Fe-Cr-Al alloys is dominated by the diffusion of oxygen ions towards the alloy surface and the outward diffusion of aluminum ions from the alloy substrate, resulting in a wavy oxide scale. When RE elements are added into the alloy, the diffusion of aluminum ions from the alloy substrate to oxide scale is suppressed. Thereby the oxidation process is dominated by the diffusion of oxygen ions towards alloy substrate, avoiding the formation of wavy scale^[17,18]. (3) RE elements tend to segregate at the grain boundaries of oxide scale. Since larger RE ions are diffused more slowly than natural cations, the normal short-circuit transport of cations along the grain boundaries is inhibited, thus reducing the growth rate of oxide scale^[19-23]. (4) Other views, such as elimination of impurities (S and C)^[24]

Received date: November 08, 2020

Foundation item: Key Research and Development Program of Jiangsu Province (BE2018097)

Corresponding author: Wu Xiaodong, Ph. D., Associate Professor, School of Materials Science and Engineering, Jiangsu University, Zhenjiang 212000, P. R. China, E-mail: wuxd@ujs.edu.cn

Copyright © 2021, Northwest Institute for Nonferrous Metal Research. Published by Science Press. All rights reserved.

and suppression of void formation at the oxide scale/alloy interface^[25], were also proposed.

In this research, an isothermal oxidation test at 1100 °C in air was conducted on Fe25Cr5Al alloys with and without RE elements La and Ce. The effects of La and Ce on the oxidation kinetics of Fe25Cr5Al alloys were studied, and those on the composition of oxide scale and the microscopic evolution mechanism were also discussed.

1 Experiment

The chemical composition of experiment materials was designed based on commercial Fe25Cr5Al alloys. The experiment materials were prepared in a vacuum melting furnace and cast into ingots of 25 kg. The raw materials consisted of high purity metals (99.9% Fe, 99.9% Cr, 99.9% Al) and the addition of RE elements La and Ce was according to the mass ratio of La:Ce≈1:4. All the specimens of 30 mm×10 mm×5 mm in size were cut from the forged alloys by wire electrode cutting machine. Fe25Cr5Al alloys with and without RE elements were named as Fe25Cr5Al-RE and Fe25Cr5Al, respectively. The chemical composition of these two alloys is listed in Table 1.

Before the oxidation tests, the specimens were ground by SiC sandpaper of 400#~2000#, and then ultrasonically cleaned in alcohol. In order to explore the change law of oxygen at the initial stage and during the long-term process, the oxidation time was set as 1, 20, and 300 h. To prevent the oxide scale from being destroyed, the specimens were embedded with epoxy resin after oxidation to observe the cross-sectional morphology.

The composition of the oxide scale was identified by X-ray diffractometer (XRD, Smart lab 9 kW, Cu K α) with the scanning speed of 5°/min. The surface morphology of the oxide scale was observed by scanning electron microscope (SEM) coupled with secondary electron (SE) mode. The cross-sectional morphology was observed by SEM coupled with backscattering electron (BSE) mode. The element distribution of the cross-section was analyzed by energy dispersive spectrometer (EDS, Octane Plus).

2 Results and Discussion

2.1 Oxidation kinetics

Oxidation kinetics curves of two alloys after oxidation at 1100 °C in air are shown in Fig.1. After oxidation for 1, 20, and 300 h, the mass gain of Fe25Cr5Al alloys is 0.08, 0.84, and 4.41 mg·cm⁻², but that of Fe25Cr5Al-RE alloys is 0.03, 0.35, and 0.92 mg·cm⁻², respectively. It can be seen that La and Ce obviously improve the oxidation resistance at high temperature of the Fe25Cr5Al alloys. In the initial stage of

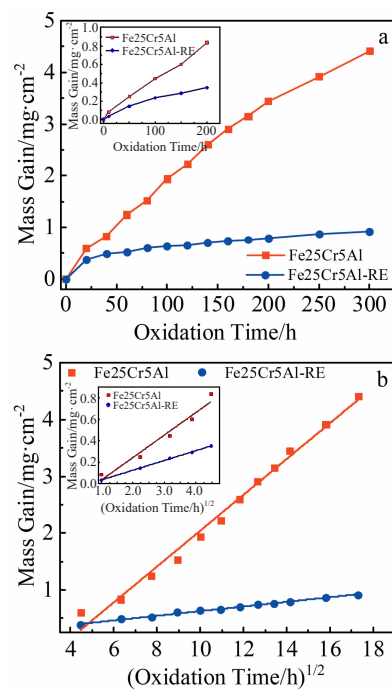


Fig.1 Oxidation kinetics curves of Fe25Cr5Al and Fe25Cr5Al-RE alloys: (a) normal plots and (b) parabolic plots

oxidation (0~20 h), the mass gain of Fe25Cr5Al alloys increases rapidly after 1 h, reaching 0.08 mg·cm⁻². However, the mass gain of Fe25Cr5Al-RE alloys is only 0.03 mg·cm⁻² after oxidation for 1 h and increases obviously after 5 h, as shown in Fig.1a. After oxidation for 300 h, the mass gain of Fe25Cr5Al alloys is 4.41 mg·cm⁻², but it is only 0.92 mg·cm⁻² for Fe25Cr5Al-RE alloys. The change trend of the mass gain of Fe25Cr5Al alloys is similar to that of other Fe-Cr-Al alloys^[26].

The oxidation resistance of alloys can be directly reflected by the oxidation rate constant, which is expressed by Eq.(1), as follows^[27].

$$\Delta(m/A) = f(\sqrt{t}) \quad (1)$$

where $\Delta(m/A)$ is mass gain per unit area, m is the mass gain, A is the area, t is oxidation time, and f represents the related function. k_0 is the parabolic rate constant ($\text{g}^2\cdot\text{cm}^{-4}\cdot\text{s}^{-1}$) and can be calculated according to the data in Fig.1b. The calculated parabolic rate constant k_0 at different stages is listed in Table 2. The linear relationship between mass gain and square root of oxidation time suggests that the all alloys obey the parabolic oxidation kinetics. During the initial stage of 0~20 h, the k_0 value of Fe25Cr5Al and Fe25Cr5Al-RE alloys is 3.5×10^{-11} and $1.5 \times 10^{-11} \text{ g}^2\cdot\text{cm}^{-4}\cdot\text{s}^{-1}$, respectively. Besides, after oxidation for 300 h, the k_0 value of Fe25Cr5Al-RE alloys decreases obviously to $6.3 \times 10^{-12} \text{ g}^2\cdot\text{cm}^{-4}\cdot\text{s}^{-1}$. However, the k_0 value of Fe25Cr5Al alloys increases slightly, reaching $5.3 \times 10^{-11} \text{ g}^2\cdot\text{cm}^{-4}\cdot\text{s}^{-1}$ after oxidation for 300 h.

Evidently, Fe25Cr5Al alloys have been oxidizing during the whole oxidation process. In contrast, the mass gain of Fe25Cr5Al-RE alloys after oxidation for 20 h basically

Table 1 Chemical composition of Fe25Cr5Al and Fe25Cr5Al-RE alloys (wt%)

Alloy	RE	Al	Cr	S	C	Fe
Fe25Cr5Al	-	5	24.7	0.007	<0.001	Bal.
Fe25Cr5Al-RE	0.031	5	24.5	0.005	<0.001	Bal.

Table 2 Parabolic rate constant k_0 of Fe25Cr5Al and Fe25Cr5Al-RE alloys after oxidation in air at 1100 °C for different durations ($\times 10^{11} \text{ g}^2 \cdot \text{cm}^{-4} \cdot \text{s}^{-1}$)

Oxidation time	0~20 h	20~300 h
Fe25Cr5Al	3.5	5.3
Fe25Cr5Al-RE	1.5	0.63

remains the same, and even slightly decreases, which indicates that a protective scale has been developed and provides excellent high temperature oxidation resistance.

2.2 Composition and microstructure of oxide scale

Fig. 2 shows the XRD patterns of oxide scales after oxidation for different durations. The strong diffraction peaks of substrate and weak peaks of $\alpha\text{-Al}_2\text{O}_3$ can be detected in both alloys after oxidation for 1 h, indicating that the oxidation degree of all alloys is not serious and few oxides are formed. In contrast, the weak peaks of substrate can be observed in Fe25Cr5Al alloys after oxidation for 300 h, while only peaks of $\alpha\text{-Al}_2\text{O}_3$ can be detected in Fe25Cr5Al-RE alloys, indicating that oxide scale of Fe25Cr5Al-RE alloys may be more compact than that of Fe25Cr5Al alloys.

The oxide scale morphologies of all alloys after oxidation at 1100 °C for 1, 20, and 300 h are shown in Fig. 3. A typical wavy scale can be observed from the surface of Fe25Cr5Al alloys, as shown in Fig. 3a~3c, which is similar to the morphology of other heat-resistant alloys containing aluminum after oxidation^[28-30]. Fig. 3b shows the surface morphology of the oxide scale after oxidation for 20 h. A few pores and cracks can be found. Furthermore, a large spalling area appears on the oxide scale of Fe25Cr5Al alloys after oxidation for 300 h, as shown in Fig. 3c. The flat and

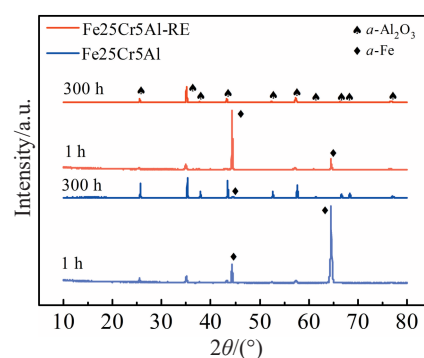


Fig.2 XRD patterns of oxide scales of Fe25Cr5Al and Fe25Cr5Al-RE alloys after oxidation in air at 1100 °C for 1 and 300 h

continuous oxide scale is formed on the surface of Fe25Cr5Al-RE alloys after oxidation, as shown in Fig. 3d~3f. The dense oxide scale (region 1 in Fig. 3d) and newly formed oxide cluster (region 2 in Fig. 3d) can be observed on the surface of Fe25Cr5Al-RE alloys after oxidation for 1 h. The morphology of oxide scale is similar to that in Ref.[31]. Pores can be found in the oxide scale of Fe25Cr5Al-RE alloy after oxidation for 20 h, but they disappear after oxidation for 300 h, as shown in Fig. 3e and 3f. However, for Fe25Cr5Al alloys after oxidation for 300 h, the pores still exist on the surface of the oxide scale (Fig. 3c), which agrees with the results in previous studies that pores are distributed on the surface of oxide scale even after long-term oxidation^[32].

Fig. 4 shows the cross-section morphologies and element distribution of Fe25Cr5Al alloys after oxidation at 1100 °C for 1, 20, and 300 h. EDS element mappings show that the components of the oxide scale are mainly composed of Al and

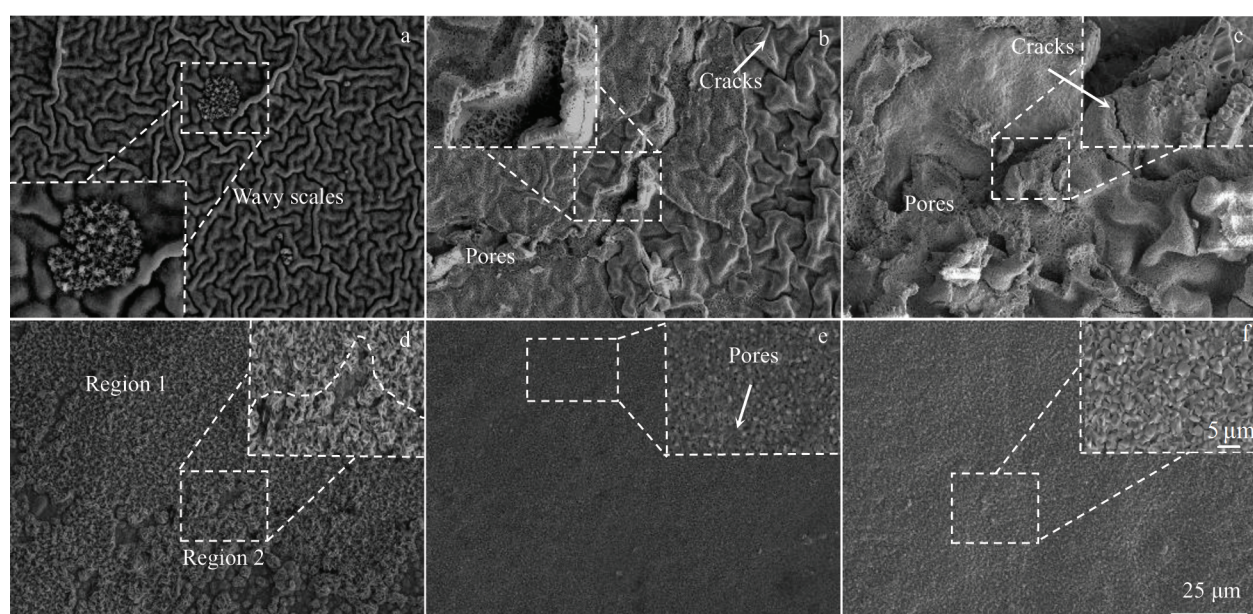


Fig.3 Morphologies of oxide scale of Fe25Cr5Al (a~c) and Fe25Cr5Al-RE (d~f) alloys after oxidation at 1100 °C for 1 h (a, d), 20 h (b, e) and 300 h (c, f)

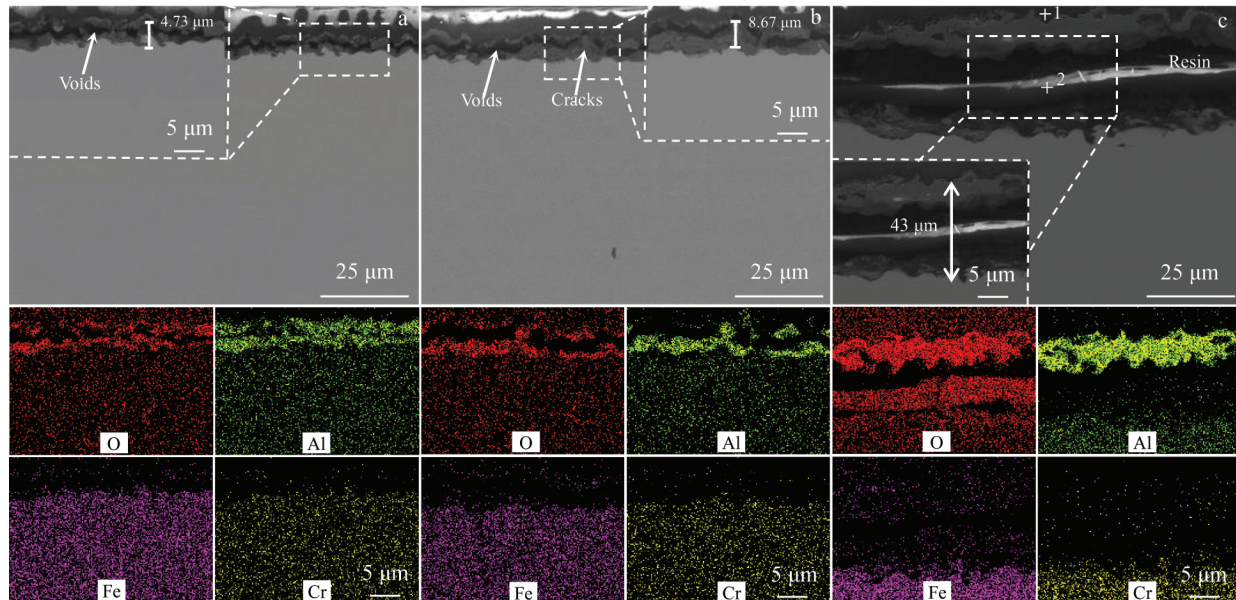


Fig.4 Cross-section morphologies and element distributions of Fe25Cr5Al alloys after oxidation at 1100 °C for 1 h (a), 20 h (b), and 300 h (c)

O elements, which is consistent with the XRD analysis. Fig.4a shows the cross-section morphology and element distributions of Fe25Cr5Al alloys after oxidation for different durations. It is obvious that the oxide scale of Fe25Cr5Al alloys has layers and many voids. The thickness of the oxide scale of Fe25Cr5Al alloys after oxidation for 1, 20, and 300 h is 4.73, 8.67, and 43 μm , respectively. An obvious oxygen-rich layer can be observed in Fig.4c, and EDS spectra in Fig.5 indicate that the layer is resin.

Fig.6 shows the compact and flat cross-section morphologies and element distributions of Fe25Cr5Al-RE alloys after oxidation at 1100 °C for 1, 20, and 300 h. After oxidation for 1 h, the thickness of the oxide scale is about 3.7 μm in some areas, while it is only about 2.18 μm in majority areas. Moreover, the thickness of the uniform and continuous oxide scale is 2.3 and 8.41 μm after oxidation for 20 and 300 h, respectively. In addition, gray-white phases can be observed at the interface between the oxide scale and substrate after oxidation for 1, 20, and 300 h. EDS analyses in Fig.7 indicate that the gray-white phases are RE oxides.

2.3 Growth mechanism of oxide scale

The oxidation kinetics curves in Fig.1 obey the parabolic rule. The overall mass gain curves of Fe25Cr5Al alloys do not completely agree with the parabolic law, but they are in accordance with the law when oxidation duration is 0~20 h. It is known that the parabolic law is based on the assumption that the oxide scale is continuous and compact. In fact, pores and cracks exist in the oxide scale, which may cause the mass gain curves to deviate from the parabolic law^[32,33]. The pores and cracks occur in the oxidation scale of Fe25Cr5Al alloys after oxidation for 20 h (Fig.3b), resulting in the fact that the mass gain curves after 20 h deviate from the parabolic law. In general, when the mass gain curves of Fe25Cr5Al alloys are consistent with the parabolic law, the oxidation reaction is dominated by diffusion. In other words, the growth of oxide scale mainly depends on the diffusion of oxygen ions into the substrate and the diffusion of metal ions away from the substrate^[34,35]. Under the same conditions of oxygen partial pressure, temperature, and oxidation time, the mass gain of

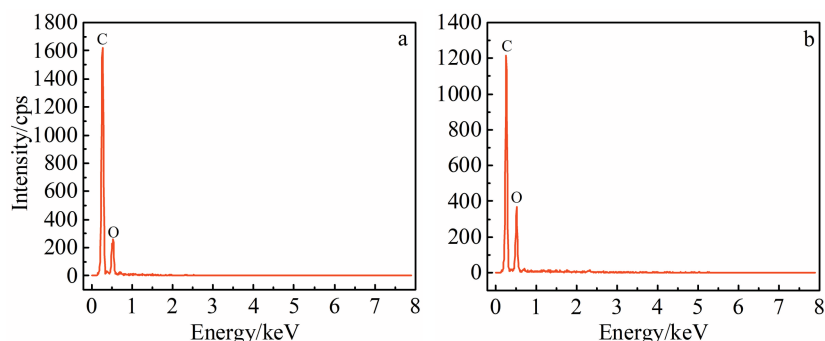


Fig.5 EDS spectra of point 1 (a) and point 2 (b) in Fig.4c

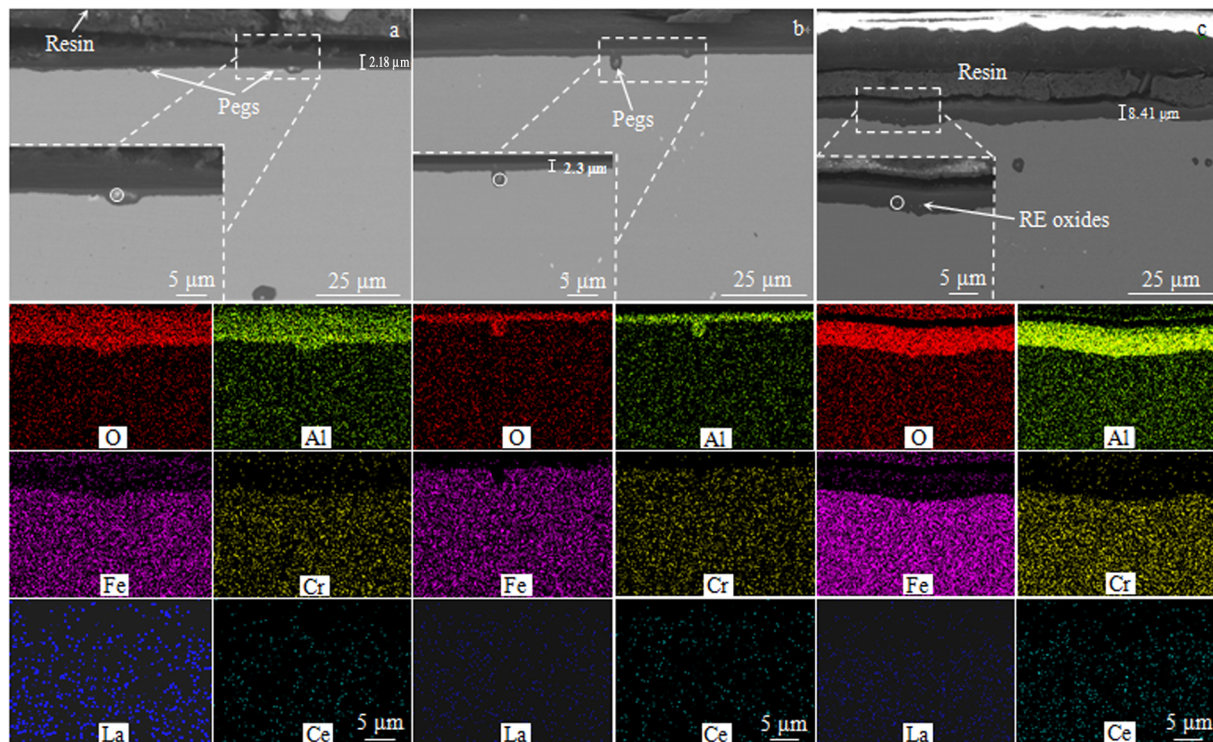


Fig.6 Cross-section morphologies and element distributions of Fe25Cr5Al-RE alloys after oxidation at 1100 °C for 1 h (a), 20 h (b), and 300 h (c)

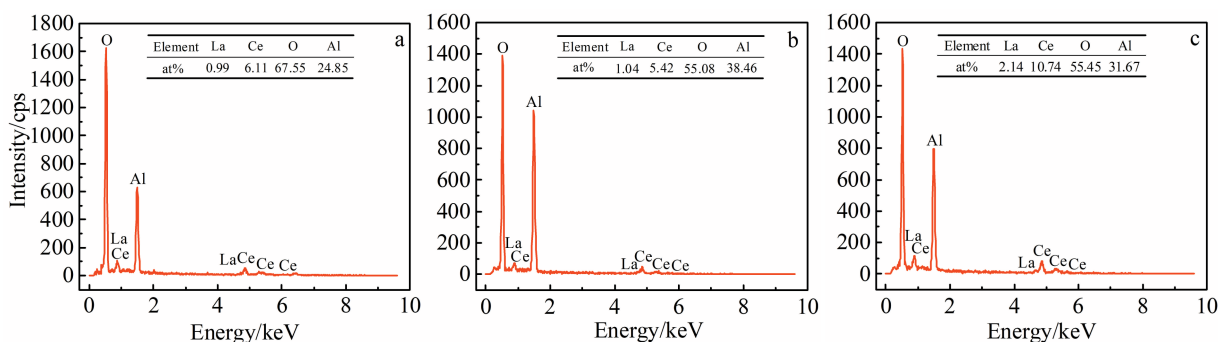


Fig.7 EDS analyses of pegs in Fig.6a (a), pegs in Fig.6b (b), and RE oxides in Fig.6c (c)

Fe25Cr5Al-RE alloys is less than that of Fe25Cr5Al alloys (Fig.1), indicating a lower oxidation rate and the formation of thinner oxide scale (Fig.4 and Fig.5). Because the addition of La and Ce is the only variables in Fe25Cr5Al alloys, it can be concluded that La and Ce affect the oxidation process of alloys by changing the ions diffusion mechanism. At the oxide scale/substrate interface, La and Ce inhibit the diffusion of Al^{3+} from the substrate to the oxide scale, resulting in the oxidation reaction in the Fe25Cr5Al-RE alloy dominated by the inner diffusion of O^{2-} ions. The addition of La and Ce significantly decreases the oxidation rate and greatly improves the adhesion of the oxide scale.

Fig. 8a shows the schematic diagram of the oxidation mechanism of Fe25Cr5Al alloy. The oxide scale of

Fe25Cr5Al alloy is wavy, and the growth mechanisms can be described as follows. The oxygen ions are diffused into the substrate surface and the aluminum ions are diffused away from the substrate, thereby forming the oxide scale. In this case, the growth stress is generated due to the formation of oxides within the oxide scale. To release the growth stress, oxide scale becomes wavy. In addition, many cracks can be observed in the oxide scale (Fig.3c), because in the cooling process, the oxide scale tends to fracture preferentially along the ridges^[19,36], eventually leading to the failure of protection mechanism of the oxide scale system.

According to Fig. 3d~3f and Fig. 6a, a compact and continuous oxide scale can be observed on the surface of Fe25Cr5Al-RE alloys. The schematic diagram of the

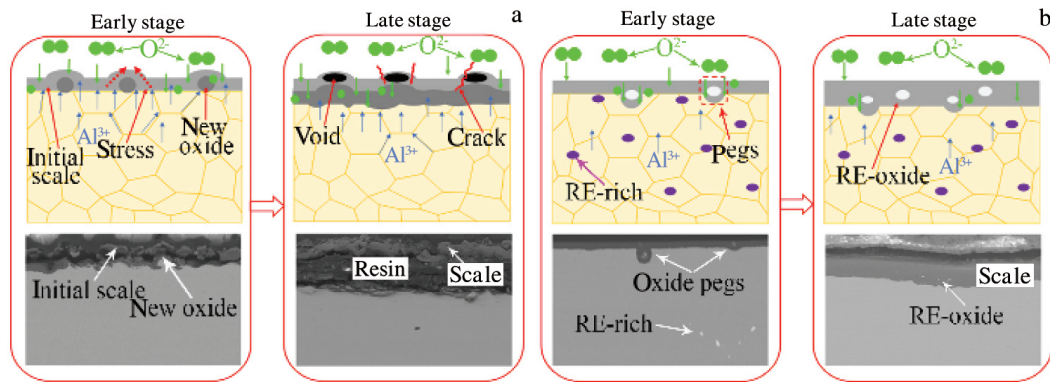


Fig.8 Schematic diagrams of growth process of oxide scale of Fe25Cr5Al (a) and Fe25Cr5Al-RE (b) alloys after oxidation at 1100 °C in air

oxidation behavior of Fe25Cr5Al-RE alloys is shown in Fig. 8b. The diffusion of aluminum ions away from the substrate is suppressed by La and Ce, and the growth mechanism of the oxide scale changes from the simultaneous diffusion of aluminum ions and oxygen ions into the simple diffusion of oxygen ions. In addition, during the oxidation process, the RE oxides formed by the oxidation reaction and RE-rich phases are distributed in the oxide scale and substrate, as shown in Fig. 6a and 6b. The oxygen ions are preferentially diffused in the substrate along the oxide channel to form the oxide pegs around RE oxides, and then the adhesion of oxide scale/substrate is strengthened, which is similar to the phenomenon in other researches of oxide pegs^[13-16]. RE oxides can be observed in the oxide scale (Fig. 6c), which may be formed by the diffusion of RE elements through the grain boundary of the oxide scale^[19-23]. In the oxidation process, the internal growth of α -Al₂O₃ causes the fact that the dispersed particles of RE oxides enter the oxide scale and a small number of RE oxides dissolve to produce RE ions which are diffused along the grain boundary of α -Al₂O₃ and react with oxygen ions, finally forming RE oxides in the oxide scale^[37]. As RE elements enter the oxide scale, the initial short-circuit transport of aluminum ions along the grain boundaries of oxide scale is suppressed.

2.4 Role of RE in oxidation process

The white spherical phases can be observed in the Fe25Cr5Al-RE alloys, as shown in Fig. 9a. EDS spectrum in Fig. 9b indicates that the spherical phases are RE-rich phase.

Compared with that of Fe25Cr5Al alloys, the mass gain of Fe25Cr5Al-RE alloys is smaller, and its oxide scale is more compact and flatter. Based on the oxidation kinetics analysis, when RE elements La and Ce are added into the alloys, the diffusion of aluminum ions from alloys to oxide scale is suppressed, resulting in the oxides formed largely at the oxide scale/substrate interface and avoiding the formation of wavy oxide scale.

Fig. 6a shows the morphology of the oxide scale of Fe25Cr5Al-RE alloys after oxidation for 1 h, and two types of α -Al₂O₃ can be observed: the dense oxides (region 1 in Fig. 3d) and newly formed oxide cluster (region 2 in Fig. 3d). The

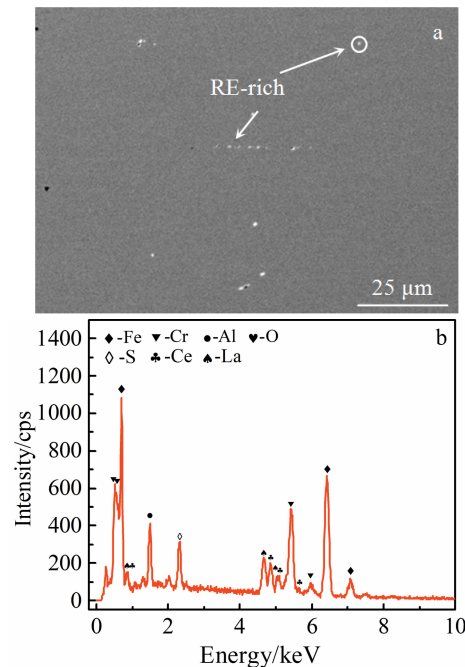


Fig.9 SEM image of Fe25Cr5Al-RE alloys before oxidation (a); EDS spectrum of RE-rich phase (b)

oxide scale of Fe25Cr5Al alloy is mainly wavy after oxidation for 1 h, and only a few fine and dense oxides can be observed, as shown in Fig. 3a. According to the oxide scale growth mechanisms, since the growth rate of the oxide scale is reduced by La and Ce during the oxidation process, La and Ce may contribute to formation of dense and uniform α -Al₂O₃ phase. In addition, a compact and flat oxide scale can effectively restrain the oxygen ions from diffusing to substrate through oxide scale. Therefore, the high temperature oxidation resistance of the Fe25Cr5Al alloys is improved significantly.

The RE oxides can be observed at the oxide scale/substrate interface, as shown in Fig. 6. In the meantime, EDS analysis shows that there are RE-rich phases in the Fe25Cr5Al-RE alloys before oxidation. In the initial stage of oxidation, the oxygen ions react with the RE-rich phases in alloys to form

RE oxides. The RE oxides may act as a short-circuit diffusion path for the oxygen ions to react with aluminum ions in the substrate, resulting in the fact that Al_2O_3 is formed around the RE oxides. As the oxidation proceeds, the Al_2O_3 around RE oxides become pegs, thereby making the oxide scale connect with the substrate more closely.

3 Conclusions

- 1) The oxide scale of Fe25Cr5Al alloys after oxidation consists of $\alpha\text{-Al}_2\text{O}_3$. Rare earth (RE)-rich phases are formed in Fe25Cr5Al alloys after RE elements La and Ce are added.
- 2) The RE elements La and Ce inhibit not only the diffusion of oxygen ions into the substrate, but also the diffusion of aluminum ions away from the substrate.
- 3) The oxygen ions are diffused into the substrate and react with the RE-rich phases in Fe25Cr5Al alloys, transforming the RE-rich phases into RE oxides.
- 4) RE oxides can act as channels for the rapid diffusion of oxygen ions, resulting in the formation of oxide pegs to enhance the adhesion between the oxide scale and the substrate. The growth of $\alpha\text{-Al}_2\text{O}_3$ results in the formation of RE oxides in the oxide scale, which is beneficial to inhibit the diffusion of aluminum ions away from the substrate into the oxide scale.

References

- 1 Wu Dongfang, Zhang Yanhong, Li Yongdan. *Journal of Industrial and Engineering Chemistry*[J], 2017, 56: 175
- 2 Kim D H, Yu B Y, Cha P R et al. *Surface and Coatings Technology*[J], 2012, 209: 169
- 3 Bai Guanghai, Xue Fei, Liu Erwei et al. *Rare Metal Materials and Engineering*[J], 2020, 49(9): 3071 (in Chinese)
- 4 Bai Guanghai, Xue Fei, Zhang Yanwei et al. *Rare Metal Materials and Engineering*[J], 2020, 49(7): 2340 (in Chinese)
- 5 Sun Z, Bei H, Yamamoto Y. *Materials Characterization*[J], 2017, 132: 126
- 6 Emmerich K. *Physica Status Solidi A*[J], 1993, 135(2): 381
- 7 Stott F H, Hiramatsu N. *Materials at High Temperature*[J], 2000, 17(1): 93
- 8 Tolpygo V K, Viehaus H. *Oxidation of Metals*[J], 1999, 52(1-2): 1
- 9 Whittle D P, Stringer J. *Philosophical Transactions of the Royal Society A*[J], 1980, 295(1413): 309
- 10 Klower J. *Materials and Corrosion*[J], 1998, 49(10): 758
- 11 Klower J. *Materials and Corrosion*[J], 2015, 51(5): 373
- 12 Dang Wei, Li Jinshan, Zhang Tiebang et al. *Rare Metal Materials and Engineering*[J], 2015, 44(2): 261
- 13 Allam I M, Whittle D P, Stringer J. *Oxidation of Metals*[J], 1978, 12(1): 35
- 14 Li Jian, Cao Guangming, Wang Hao. *Corrosion Science*[J], 2020, 174: 108 796
- 15 Ramanarayanan T A, Raghavan M, Petkovic-Luton R. *Oxidation of Metals*[J], 1984, 22(3-4): 83
- 16 Mennicke C, He M Y, Clarke D R et al. *Acta Materialia*[J], 2000, 48(11): 2941
- 17 Fountain J G, Golightly F A, Stott F H et al. *Oxidation of Metals*[J], 1976, 10(5): 341
- 18 Golightly F A, Wood G C, Stott F H. *Oxidation of Metals*[J], 1980, 14(3): 217
- 19 Pint B A. *Oxidation of Metals*[J], 1996, 45(1-2): 1
- 20 Luthra K L, Briant C L. *Oxidation of Metals*[J], 1986, 26(5-6): 397
- 21 Ramanarayanan T A. *Journal of the Electrochemical Society*[J], 1984, 131(4): 923
- 22 Jedliński J, Grosseau-Poussard J L, Kowalski K et al. *Oxidation of Metals*[J], 2013, 79(1-2): 41
- 23 Kim D E, Shang S L, Li Z et al. *Oxidation of Metals*[J], 2019, 92(3-4): 303
- 24 Hou P Y. *Journal of the American Ceramic Society*[J], 2003, 86: 660
- 25 Quadakkers W J, Naumenko D, Pint B A. *Oxidation of Metals*[J], 2016, 86(4): 660
- 26 Hiramatsu N, Stott F H. *Oxidation of Metals*[J], 1999, 51(5-6): 479
- 27 Issartel C, Buscail H, Chevalier B et al. *Oxidation of Metals*[J], 2017, 88(1-2): 1
- 28 Choi H, Yoon B, Kim H et al. *Surface and Coatings Technology*[J], 2002, 150(2-3): 297
- 29 Mahesh R A, Jayaganthan R, Prakash S. *Surface Engineering*[J], 2011, 27(5): 332
- 30 Yang Zhi, Pan Jie, Wang Zixie et al. *Corrosion Science*[J], 2020, 172: 108 728
- 31 Ju Jiang, Yang Chao, Ma Shengqiang et al. *Corrosion Science*[J], 2020, 170: 108 620
- 32 Zheng Zhibin, Wang Shuai, Long Jun et al. *Corrosion Science*[J], 2020, 164: 108 359
- 33 Wei Liangliang, Zheng Jiahao, Chen Liqing et al. *Corrosion Science*[J], 2018, 142: 79
- 34 Huntz A M. *Journal of Materials Science Letters*[J], 1999, 18(24): 1981
- 35 Cao J D, Zhang J S, Hua Y Q et al. *Rare Metals*[J], 2017, 36(11): 878
- 36 Stott F H, Golightly F A, Wood G C. *Corrosion Science*[J], 1979, 19(11): 889
- 37 Wang X, Peng X, Tan X et al. *Scientific Reports*[J], 2016, 6: 29 593

镧和铈对 Fe25Cr5Al 合金高温氧化行为的影响

吴晓东¹, 王联进¹, 王忠英², 陈雪琴¹, 王 双¹

(1. 江苏大学材料科学与工程学院, 江苏 镇江 212000)

(2. 钢铁研究总院淮安有限公司, 江苏 淮安 223000)

摘要: 含稀土元素 La、Ce 的 Fe25Cr5Al-RE 合金和不含稀土的 Fe25Cr5Al 合金在 1100 °C 的空气中进行了恒温氧化实验。采用扫描电子显微镜 (SEM) 观察氧化膜形貌, 使用 X 射线衍射仪 (XRD) 结合能谱仪 (EDS) 分析氧化膜成分。结果表明, 氧化 1、20 和 300 h 后, Fe25Cr5Al 合金增重分别为 0.08、0.84 和 4.41 mg·cm⁻², Fe25Cr5Al-RE 合金增重分别为 0.03、0.35 和 0.92 mg·cm⁻²。氧化后所有合金的氧化膜成分均为 α -Al₂O₃。La、Ce 能够促进合金形成致密、连续的氧化膜, 显著提高了 Fe25Cr5Al 合金的抗高温氧化性能。此外, Fe25Cr5Al-RE 合金氧化膜/基体界面存在稀土氧化物钉, 使得氧化膜与基体的结合更加紧密, 增强了氧化膜/基体粘附性。Fe25Cr5Al-RE 合金氧化后, 氧化膜内存在稀土氧化物, 有效地防止了合金发生进一步氧化。

关键词: 氧化机理; Fe-Cr-Al 合金; 氧化膜

作者简介: 吴晓东, 男, 1969 年生, 博士, 副教授, 江苏大学材料科学与工程学院, 江苏 镇江 212000, E-mail: wuxd@ujs.edu.cn